



1 **Wetter environment and increased grazing reduced the area burned in northern Eurasia: 2002 –**  
2 **2016**

3 Wei Min Hao<sup>1</sup>, Matthew C. Reeves<sup>2</sup>, L. Scott Baggett<sup>3</sup>, Yves Balkanski<sup>4</sup>, Philippe Ciais<sup>4</sup>, Bryce  
4 L. Nordgren<sup>1</sup>, Alexander Petkov<sup>1</sup>, Rachel E. Corley<sup>1</sup>, Florent Mouillot<sup>5</sup>, Shawn P. Urbanski<sup>1</sup>,  
5 Chao Yue<sup>6</sup>

6  
7 <sup>1</sup>United States Forest Service, Rocky Mountain Research Station, Fire Sciences Laboratory, 5775  
8 Highway 10 West, Missoula, MT 59808 USA.

9 <sup>2</sup>United States Forest Service, Rocky Mountain Research Station, Forestry Sciences Laboratory,  
10 800 E. Beckwith, Missoula, MT 59801, USA.

11 <sup>3</sup>United States Forest Service, Rocky Mountain Research Station, 240 West Prospect, Fort  
12 Collins, CO 80526, USA.

13 <sup>4</sup>Laboratoire des Sciences du Climat et de l'Environnement, LSCE CEA CNRS UVSQ, 91191  
14 Gif Sur Yvette, France.

15 <sup>5</sup>UMR CEFE 5175, Centre National de la Recherche Scientifique (CNRS), Université de  
16 Montpellier, Université Paul-Valéry Montpellier, Ecole Pratique des Hautes Etudes (EPHE),  
17 Institut de Recherche pour le Développement, 34293 Montpellier CEDEX 5, France.

18 <sup>6</sup>Institute of Soil and Water Conservation, Northwest A&F University, Yangling, Shaanxi  
19 712100, P.R. China.

20

21 **Correspondence:** Wei Min Hao ([weimin.hao@usda.gov](mailto:weimin.hao@usda.gov))

22

23 **Abstract.** Northern Eurasia is highly sensitive to climate change. Fires in this region can have  
24 significant impacts on regional air quality, radiative forcing and black carbon deposition in the  
25 Arctic to accelerate ice melting. Using a MODIS-derived burned area data set, we report that the  
26 total annual area burned in this region declined by 53 % during the 15-year period of 2002–2016.  
27 Grassland fires dominated the trend, accounting for 93 % of the decline of the total area burned.  
28 Grassland fires in Kazakhstan contributed 47 % of the total area burned and 84% of the decline.  
29 Wetter climate and increased grazing are the principle driving forces for the decline. Our  
30 findings: 1) highlight the importance of the complex interactions of climate-vegetation-land use  
31 in affecting fire activity, and 2) reveal how the resulting impacts on fire activity in a relatively  
32 small region such as Kazakhstan can dominate the trends of burned areas across a much larger  
33 landscape of northern Eurasia. Our findings may be used to improve the prediction of future fire  
34 dynamics and associated fire emissions in northern Eurasia.

35 **1 Introduction**

36 Fire activity worldwide is very sensitive to climate change and human actions, especially over  
37 high latitude ecosystems (Goetz et al., 2007). Identifying and unraveling confounding fire drivers  
38 is critical for understanding the recent and future impacts of fire activity. In northern Eurasia fire  
39 activity impacts of chief concern include carbon cycling, boreal ecosystem dynamics, fire  
40 emissions (Hao et al., 2016a), accelerated ice melting in the Arctic (Hao et al., 2016a;  
41 Evangeliou et al., 2016), early thawing of permafrost, the hydrological cycle of high-latitudes  
42 (IPCC, 2014), and air quality in Europe, Asia and North America. An improved understanding of  
43 the region's fire dynamics can also be applied to develop climate change mitigation policy and



44 be incorporated into the fire modules of Earth System Models to improve their predictions  
45 (Hantson et al. 2016).

46 Global mean surface temperature rose by approximately 0.72° C from the year 1951 to 2012  
47 according to the 5<sup>th</sup> Intergovernmental Panel on Climate Change Report (IPCC) (IPCC, 2013),  
48 but remained relatively constant (“warming hiatus”) from 1998 to 2013 (Fyfe et al., 2013;  
49 Cowtan and Way, 2014; Trenberth et al., 2014). Nevertheless, extreme high temperature events  
50 continued to occur even during the warming hiatus (Seneviratne et al., 2014; Trenberth et al.,  
51 2015). Since 2013, the global temperatures have risen rapidly (NASA Global Climate Change,  
52 2019). High latitudes are projected to have the largest temperature increase globally by 2100  
53 (IPCC, 2013). At the same time, however, components of the fire weather index (FWI), an index  
54 of fire intensity potential, have experienced regional divergence at these latitudes with a positive  
55 FWI trend in Eastern Asia and a negative trend in Kazakhstan (Jolly et al. 2015), suggesting  
56 divergent regional climate impacts.

57 Northern Eurasia, defined here as a region from 35° N to the Arctic and from the Pacific Ocean  
58 to the Atlantic Ocean, comprises 21 % of the Earth’s land area and encompasses diverse  
59 ecosystems from the steppes of central Asia to the Arctic. Forest is the major ecosystem covering  
60 an area of 27 % in northern Eurasia (Friedl et al., 2010), followed by grassland of 16 %. Over the  
61 past 20 years, the decline of total area burned in Eurasia has been observed by Giglio et al.,  
62 2013; Hao et al., 2016a and Andela et al., 2017.

63 Fire activity is greatly influenced by climate, fuels and human activity in different ways over  
64 different ecosystems (e.g. Pausas and Ribeiro, 2013; Andela et al., 2017). Considerable research  
65 has been done to understand climate-fire-grazing interactions in grassland ecosystems. In  
66 grasslands reductions in fuel availability due to decreasing net primary production, grazing, or  
67 other management activities can be the key variables limiting fire spread (Moritz et al., 2005). In  
68 the western United States, the research has significant implications on forest and rangeland  
69 management (e.g. Bachelet et al., 2000; Gedalof et al., 2005; Riley et al., 2013; Abatzoglou and  
70 Kolden, 2013). Similar issues were investigated on African savanna for maintaining sustainable  
71 grassland (e.g. Archibald et al., 2009; Koerner and Collins, 2014). In this study we closely  
72 examine the interactions of climate, fire, grazing and fuel availability in the region of northern  
73 Eurasia with the largest decline in burned area during 2002–2016.

74 To disentangle keystone variables affecting fire activity, we examined the trends of the spatial  
75 and temporal distribution of the area burned from 2002 to 2016 across different land cover types  
76 and geographic regions of northern Eurasia. Daily NASA MODIS (**M**oderate Resolution  
77 **I**maging **S**pectroradiometer) dataset at a 500 m × 500 m resolution was used. The burned area  
78 data were analyzed at multiple spatial and temporal scales using frequentist statistical methods to  
79 identify the regional trends. We identified the geographic region with the largest declining trend  
80 and explore the influence of the confounding factors of climate and human activity on burned  
81 area in this region. Assessing burned area changes in northern Eurasia over this time period  
82 benefits from the lack of fire suppression in this region (Goldammer et al., 2013), so the impact  
83 of climate and land use on fire activity can be better understood.



## 84 **2 Methodology**

### 85 **2.1 Mapping burned areas**

86 Since the year 2000, global burned area has been mapped by remote sensing (e.g. Mouillot et al.  
87 2014) with different sensors and detection algorithms (Chuvienco et al., 2019), leading to multiple  
88 datasets with a significant uncertainty in the magnitude of spatial distribution, interannual  
89 variability and trends in burned area (Hantson et al. 2016). Our methodology used for mapping  
90 daily burned area is very similar to that used by Hao et al. (2016a, 2016b), with the only  
91 difference being the land cover product. This study used annual edition of land cover/land cover  
92 change product (MCD12) for 2002–2013 and the land cover map for 2013 was used for the years  
93 of 2014–2016 because current versions were not available. The study of Hao et al. (2016a,  
94 2016b) used the MCD12 land cover map of 2005 for all years. This study used the land cover  
95 map for collection 5 (Friedl et al., 2010) which was no longer available for download. The  
96 methodology has been validated in eastern Siberia (Hao et al., 2016a). The Forest Service Fire  
97 Emission Inventory – Northern Eurasia (FEI-NE) burned area dataset has been used to estimate  
98 black carbon emissions in northern Eurasia and their transport and deposition to the Arctic (Hao  
99 et al., 2016a; Evangelidou et al., 2016).

### 100 **2.2 Data sources of drought, land cover and livestock**

101 We will describe the data sources for estimating the factors affecting the burned area in  
102 Kazakhstan: drought, land cover, ecosystem productivity and livestock density. All data were  
103 evaluated at the county level for 174 counties during the period of 1992–2016 (Fig. 1). We  
104 focused on Kazakhstan as the region with the largest decline of burned area in northern Eurasia  
105 (see section 3.1).

#### 106 **Drought**

107 The Palmer Drought Severity Index (PDSI) from the TerraClimate site  
108 (<http://www.climatologylab.org/>) was used to estimate drought throughout the study area. The  
109 PDSI was developed by Palmer (1965) and is widely used to estimate a rough soil water budget  
110 based on monthly precipitation, potential evapotranspiration with varying soil property of  
111 available water content to account for pedological variations and species roots access to water.  
112 Among the monthly PDSI values available, we used monthly PDSI data from March to July,  
113 defined as the fire season (Roy et al., 2008), to compute a cumulative drought effect index from  
114 March to July in 2002–2016. The gridded PDSI data were available at a spatial resolution of ~ 4  
115 km and were aggregated to the 174 counties within the study area (Fig. 1). PDSI varies from +4  
116 for wet conditions to -4 for dry conditions.

#### 117 **Livestock**

118 The annual population of livestock in each of the 14 provinces of Kazakhstan from 2002 to 2016  
119 were compiled by the official agriculture statistics of the Ministry of National Economy of the  
120 Republic of Kazakhstan Committee on Statistics (MANE 2019). These data included yearly  
121 numbers of large horned livestock and sheep and goats at the province level which is coarser



122 than the counties. Livestock populations are only available at the province level and the  
123 population was distributed proportionally to the size of the county area so that all potential  
124 drivers of fire activity could be evaluated on a common spatial scale. The livestock density for  
125 each county is defined as the ratio of the number of animals to the size of the county.

### 126 Annual Biomass Production

127 We estimated the annual biomass production within the grassland domain of the study area (Fig.  
128 2) using the production subroutine of the Rangeland Vegetation Simulator model (RVS) (Reeves  
129 2016). The RVS, which was originally developed for simulating rangeland vegetation dynamics  
130 in the continental United States, models annual production based on MODIS normalized  
131 difference vegetation index (NDVI) at a 250 m spatial resolution (MOD13Q1). The MOD13Q1  
132 NDVI data are composited on a bi-weekly basis and are available at a spatial resolution of 250  
133 m. The QA/QC flags were used to isolate only the best quality NDVI pixels. The conversion of  
134 NDVI to aboveground net primary production (ANPP) for non-forest environments in the RVS  
135 is divided into two groups to enable different models to be fit to the lower and upper end of  
136 production given as

$$137 \quad \text{ANPP} = 240.31 * e^{3.6684(X)} \quad (1)$$

138 where estimated ANPP is in lbs ac<sup>-1</sup> of dry weight and X is the annual maximum NDVI for the  
139 upper range ( $X \geq 0.46$ ) and

$$140 \quad \text{ANPP} = 971.1 * \ln(X) + 1976 \quad (2)$$

141 where X is the annual maximum NDVI for the lower range ( $X < 0.46$ ).

### 142 Land Cover

143 The MODIS land cover product (MOD12Q1) Version 6.0 was used to assess factors affecting  
144 the burned area in Kazakhstan. The product is available at a 500 m spatial resolution and  
145 describes the distribution of broad vegetation types. We screened these data to subset only those  
146 vegetation types considered to represent grassland vegetation (Class 10 in the MOD12Q1  
147 dataset) from 2000 to 2016.

### 148 Statistical Analysis

149 For each pixel of  $0.5^\circ \times 0.5^\circ$ , the annual trend was estimated as the robust linear slope computed  
150 from burned area on year using M-estimation as described in Huber (1981). The trends were  
151 estimated using the R platform (R Core Team, 2019) with R function *rlm* in package MASS  
152 (Venables and Ripley, 2002). Pairwise robust rank correlations were computed as described in  
153 Kendall (1938) using the R function *cor*.

154 To validate our estimates on burned areas, we compare of our annual northern Eurasia burned  
155 areas (FEI-NE) with the latest version of the MODIS burned area product (MCD64A1, collection  
156 6) (Giglio et al., 2018) from 2002 to 2016. The burned areas reported by FEI-NE and MODIS  
157 MCD64 were each modeled separately by year. The models each include a first-order  
158 autoregressive term on the residuals to account for the presence of temporal autocorrelation. The



159 response was assumed to be gamma distributed. A generalized linear mixed model (GLMM)  
160 approach was used and estimated using the R function *glmmTMB* in platform (R Core Team,  
161 2019) with R package *glmmTMB* (Brooks et al., 2017).

162 The potential driving forces of burned area at the county level of 174 counties over a period of  
163 15 years from 2002 to 2016 were modeled using frequentist to interpret the effects on the extent  
164 of the area burned. The proportion of burned area per county was modeled on the effects of year,  
165 PDSI during the fire season (May-July), proportion of grass area, ANPP and livestock density  
166 along with two-way interactions. The model included a random effect that accounts for spatial  
167 correlation within each region along with a first-order autoregressive term on the residuals within  
168 each county that accounts for temporal autocorrelation. The response was assumed to be beta  
169 distributed. A generalized linear mixed model (GLMM) approach was used and estimated using  
170 the R platform (R Core Team, 2019) with R package *glmmTMB* (Brooks et al., 2017).

### 171 **3 Results**

#### 172 **3.1 Spatial and temporal distribution of burned areas**

173 The declining trends in the spatial distribution of the area burned from 2002 to 2016 in northern  
174 Eurasia at a  $0.5^\circ \times 0.5^\circ$  resolution are shown in Fig. 2. The majority of the area burned in the 15  
175 years was grassland of Kazakhstan in central Asia. However, substantial areas were also burned  
176 in the Russian Far East along the Chinese border because of illegal logging (Vandergert and  
177 Newell, 2003) and the subsequent fires to burn the remaining forest residues. The annual areas  
178 burned according to ecosystem and geographic region are summarized in Table 1. The  
179 interannual burned area in northern Eurasia varied about four times within a range from  $1.2 \times 10^5$   
180  $\text{km}^2$  in 2013 to  $5.0 \times 10^5 \text{ km}^2$  in 2003 with an average of  $(2.7 \pm 1.0) \times 10^5 \text{ km}^2$  ( $n = 15$ ). Grassland  
181 accounted for 71 % of the total area burned, despite comprising only 16 % of the land cover  
182 (Friedl et al., 2010). Almost all the grassland fires occurred in Kazakhstan in central and western  
183 Asia (Table 1). In contrast, forest is the major ecosystem that covers 27 % of northern Eurasia  
184 (Friedl et al., 2010), but contributes only 18 % of the total area burned. About ninety percent of  
185 the forest area burned occurred in Russia.

#### 186 **3.2 Trends of burned areas**

187 Comparisons of our annual northern Eurasia burned areas (FEI-NE) with the latest version of the  
188 MODIS burned area product (MCD64A1, collection 6) (Giglio et al., 2018) from 2002 to 2016  
189 are shown in Fig. 3. The burned areas in these two datasets agree better in recent years after  
190 2010. Both FEI-NE and MCD64A1 demonstrated declining trends and similar interannual  
191 variability. The FEI-NE dataset was used to analyze the driving forces for the decline of burned  
192 area in Kazakhstan (see sections 3.3–3.4).

193 Grasslands of Kazakhstan dominate the changes of the burned area with significant declines  
194 mostly in central and northern Kazakhstan, adjacent to the Russian border. The temporal trend of  
195 annual burned areas over all vegetation types and in grasslands in northern Eurasia and in  
196 Kazakhstan from 2002 to 2016 are shown in Fig. 4. The burned area trends shown in Fig. 4 were  
197 modeled like that reported in Fig. 3 with the same response distribution. The annual total area  
198 burned over northern Eurasia during this period decreased by 53 % from  $3.3 \times 10^5 \text{ km}^2$  in 2002 to



199  $1.6 \times 10^5 \text{ km}^2$  in 2016 (Table 1), or at a rate of  $1.2 \times 10^4 \text{ km}^2$  (or 3.5 %)  $\text{yr}^{-1}$ . The grassland area  
200 burned during the 15 years declined by 74 % from  $2.8 \times 10^5 \text{ km}^2$  in 2002 to  $7.3 \times 10^4 \text{ km}^2$  in  
201 2016, or at a rate of  $1.3 \times 10^4 \text{ km}^2$  (or 4.9 %)  $\text{yr}^{-1}$ . Grassland fires in Kazakhstan accounted for 47  
202 % of the total areas burned but contributed 84 % of the declining trend. The annual forest burned  
203 area varied by a factor of 5 from  $21,243 \text{ km}^2$  in 2010 to  $111,019 \text{ km}^2$  in 2003, but there is no  
204 trend over the 15 years (Table 1).

205

### 206 3.3 Regional trends in driving forces over time

207 One of our objectives was to evaluate trends in the primary drivers responsible for reducing area  
208 burned, especially in grasslands at the county level. Pairwise correlation results are shown in Fig.  
209 5. Each panel of Fig. 5 illustrates the coefficient of correlation between a key variable and year  
210 (2002–2016) for the 174 counties of Kazakhstan. The major factors affecting the trend of area  
211 burned in Kazakhstan are wetter climate (represented as PDSI), the proportion of grassland  
212 cover, ANPP and livestock density (Table 2). Grassland enables spreading fires and ANPP  
213 enables sustaining fires.

214 The declining trends in the fraction of the area burned annually are shown in Fig. 5a. The trend  
215 of PDSI from March to July during the 15-year period is illustrated in Fig. 5b. A higher PDSI  
216 value indicates a wetter environment. Increasing wetness, i.e. higher PDSI, during the fire season  
217 reduces the probability of fire ignition and fire spread. The declining trend of the burned area  
218 (Fig. 5a) is then consistent of the increasing trend of PDSI (wet conditions) especially in central  
219 and southern Kazakhstan (e.g. East Kazakhstan, Qaraghandy, Zhambyl, Almaty) (Fig. 5b).

220 Through time the proportion of grassland cover has been asymmetric with some counties having  
221 exhibited strong decreases such as in the north central region of Kazakhstan, while others have  
222 seen increases such as in the north western region (Fig. 5c). This north central region has also  
223 exhibited decreases in burned area (Fig. 5a). Similarly, some regions have shown increasing  
224 trends of grassland cover through time without commensurate increases in the proportion of  
225 burned area (Figs. 5a and 5c).

226 The impacts of year, PDSI, grassland layer, ANPP and livestock density on the extent of the area  
227 burned and the correlations of burned area with these driving forces are illustrated in Fig. 6. Area  
228 burned and PDSI were negatively correlated in most of the counties in Kazakhstan (Fig. 6b).  
229 Therefore, as Kazakhstan becomes wetter during the fire season, the area burned declined over  
230 the 2002–2016 period. At the same time, grassland cover decreased across most of Kazakhstan,  
231 with a notable exception being the north central region and south western region (Fig. 6c). ANPP  
232 decreased with time over most of Kazakhstan, the exception being central and south western  
233 counties (Fig. 6d).

234 Finally, we investigated livestock density as a potential non-climatic driver affecting fuel  
235 amount. The population density of livestock increased with time in all counties and was greatest  
236 in the central, northern and southern counties of Qostanay, Pavlodar and Qaraghandy (Fig. 5e).  
237 The coupling of livestock density with PDSI affected the extent of the area burned (Fig. S1.4)  
238 with  $p = 0.042$  (Table 2). The area burned was negatively correlated with the population of  
239 livestock throughout nearly all of Kazakhstan (Fig. 6e). This observation suggests the increasing  
240 population of grazing livestock may have reduced fuelbed continuity leading to the decrease of



241 the area burned in Kazakhstan. Since 2000, the numbers of sheep, goats and cattle have increased  
242 by 60% in Kazakhstan based on MANE statistics (2019), respectively (Figs. S2 and S3). Thus,  
243 increased livestock grazing could decrease the amount of herbaceous fuel across the landscape  
244 and offset increases in fuel quantity due to expanded grassland cover. The net result would be  
245 reductions in fire spread and the area burned.

### 246 **3.4 Interactions of driving forces**

247 The driving forces (e.g. year, PDSI, proportion of grassland cover, ANPP, livestock density) for  
248 the decline of the burned areas in Kazakhstan from 2002 to 2016 are inter-related. It is therefore  
249 critical to evaluate their interactions. For instance, Figures S1.1–S1.4 illustrate the proportion of  
250 burned area is affected by the interactions of the driving forces at 174 counties over 15 years in  
251 Table 2.

252 **Proportion of grassland cover and year** Both year and the proportion of grassland area had  
253 significant effects on burned area when interacted (Table 2,  $p < 0.001$ ). While the proportion of  
254 grassland cover in a county is very low (e.g. 0.48 %), only about 0.6 % of the area was burned  
255 annually during the period of the year 2002 to 2016 (Fig. S1.1, upper left panel). On the contrary,  
256 while the grassland cover is 25 %, the area burned declined steadily from 1.5 % in the year 2000  
257 to 0.6 % in 2016 (Fig. S1.2 lower right panel). This observation is consistent with grassland  
258 enhancing the spread of fires in the absence of opposing factors.

259 **PDSI and proportion of grassland area** Both PDSI and the proportion of grassland area had  
260 significant effects on burned area when interacted (Table 2,  $p = 0.028$ ). As in Fig. S1.2, for PDSI  
261 in a range of  $-4.5$  to  $\sim 2$ , the percentage of the area burned remained about 0.6 % for grassland  
262 area of 0.5 % (upper left panel). On the other hand, when grassland cover of 60 %, the fraction of  
263 area burned declined from 2.2 % to 0.8 % (lower right panel). This analysis is consistent with  
264 grassland enhancing the spread of fires, as in the previous section of proportion of grassland  
265 cover through time, and illustrates that increasing wetness significantly decreases burned area  
266 mostly when grassland cover is high.

267 **Livestock density and year** We investigated livestock density as a potential non-climatic driver  
268 affecting fuel amount and area burned. The effects of grazing on the area burned during 2002 –  
269 2016 are shown in Table 2,  $p = 0,089$ . The declining trend of the area burned with time for  
270 different livestock density are illustrated in Fig. S1.3. The higher the livestock density resulting  
271 in less available biomass to burn, the less area burned (lower right panel). It provides additional  
272 evidence that grazing could reduce the area burned in Kazakhstan.

273 **PDSI and livestock density** The interaction between PDSI and livestock was significant to  
274 affect the area burned ( $p = 0.042$ ). Figure S1.4 shows the decline in the proportion of burned area  
275 with PDSI at different livestock densities. As PDSI increases (wetter landscape), less area is  
276 burned. However, the declining trends differ with livestock density. This relationship is quite  
277 different for the livestock density of 0.002 heads  $\text{km}^{-2}$  (Fig. S1.4 upper left panel) and 0.05 heads  
278  $\text{km}^{-2}$  (Fig. S1,4 lower right panel). For instance, for low PDSI ( $-4$ , dry), 1.5 % of the area was  
279 burned for all livestock densities. On the contrary, at high PDSI ( $+2$ , wet), the percentage of  
280 burned area decreased with increasing livestock density. Thus, during dry years the area burned



281 is unaffected by grazing intensity, but during wet years with high biomass (based on our RVS  
282 analysis of Reeves, 2016), high grazing intensity tends to decrease burned area.

## 283 **4 Discussion**

### 284 **Burned area**

285 The spatial and temporal extent of the area burned were examined in different ecosystems in  
286 northern Eurasia during 2002 to 2016, during which the average area burned was  $(2.7 \pm 1.0) \times 10^5$   
287  $\text{km}^2 \text{ yr}^{-1}$ . The burned area in grasslands declined 74 % from  $\sim 282,000 \text{ km}^2$  in 2002 to  $\sim 73,000$   
288  $\text{km}^2$  in 2016 at a rate of  $1.3 \times 10^4 \text{ km}^2 \text{ yr}^{-1}$ . The area burned in forest showed no trend over time.  
289 Our burned area is higher than the MODIS MCD64 collection 6, in which the average annual  
290 burned area was  $9.7 \times 10^4 \text{ km}^2$  in boreal Asia during the same period (Giglio et al., 2018).  
291 Boreal Asia of MCD64 has a similar geographic region as our northern Eurasia. Nevertheless,  
292 the interannual variability and the trends of burned area for the two datasets are consistent (Fig.  
293 3).

294 Our results on burned area trends are also consistent with other published results (Giglio et al.,  
295 2013; Hao et al., 2016a; Andela et al., 2017) that concluded the area burned in northern Eurasia  
296 declined, contrary to the projections of increased fire frequency driven by climate change  
297 (Groisman et al., 2007; Kharuk et al., 2008). Uncertainty in global burned area remains a critical  
298 challenge with high variability on trends and interannual variability between sensors and  
299 processing algorithms (Hantson et al., 2016; Chuvieco et al., 2019).

### 300 **Grassland fires and grazing**

301 Grassland fires in Kazakhstan accounted for 47 % of the total area burned but comprised 84 % of  
302 the decline of the total area burned in northern Eurasia during the 15 years of 2002–2016. The  
303 grassland fires are human caused to produce fresh grass for grazing (Lebed et al., 2012) with a  
304 cycle of about every two years. A similar temporal pattern characterizes grassland fire  
305 occurrence in the African savanna (Hao and Liu, 1994; Andela and van der Werf, 2014).

306 Central Asia experienced tremendous socioeconomic change, with the collapse of the Soviet  
307 Union in the 1990's leading to a full restructure of the agricultural system, followed by a rapid  
308 collapse of cattle industry and progressively recovered in the last 20 years, and potentially  
309 altering fuel availability to burn as observed in other ecosystems (Holdo et al. 2009, Vigan et al.  
310 2017) (Figs. S2 and S3) (Food and Agriculture Organization, 2016; Robinson and Milner-  
311 Gulland, 2003). The coincident decline in burned area with increasing livestock population  
312 suggests changing agricultural practices may have exerted an influence on fire activity in  
313 Kazakhstan and northern Eurasia. In addition, the relationship between livestock population and  
314 the burned area was observed in arid grassland in a small region of southern Russia from 1986 to  
315 2006 (Dubinin et al., 2011). During this time period, the livestock population was negatively  
316 correlated with the area burned.

317 The fire activity data for Kazakhstan and Mongolia can be estimated from 1985 to 2017 as shown  
318 in Fig. 7 based on the recently released AHVRR long term fire history (Oton et al. 2019). This  
319 new information extends the analysis before our observed decrease during the 2002–2016 period  
320 and shows that fire activity increased in Kazakhstan just during the economic collapse and the





321 associated reduction of livestock in the year 2000. This opposite trend supports our interpretation  
322 on the relationship between grazing and burned area, particularly when this variation in burned  
323 area is not clearly observed in neighboring Mongolia where grazing collapse did not occur.

324 In the steppe of neighboring Mongolia, overgrazing also affected fire activity from 1988–2008  
325 (Liu et al., 2013) in a manner similar to Kazakhstan. However, extreme winter freezing and  
326 inadequate preparation affected the increasing livestock trend driven by the poorly prepared  
327 feeding of hay and foliage. It led to livestock reductions during the colder season than the  
328 average period during the years of 2000 to 2014 (Nandintsetseg et al. 2018), highlighting the  
329 potential impact of climate on livestock population beside human decisions and practices (Xu et  
330 al., 2019).

### 331 **Modelling fire and grazing interactions**

332 Accounting for confounding factors related to burned area and the subsequent effects on  
333 ecosystems, biosphere/atmosphere interactions and climate have been a challenge in developing  
334 fire modules in global vegetation models (Hantson et al. 2016). Climate (drought, temperature  
335 and humidity), land cover and fuel amount are the main drivers related to fire activity in  
336 Dynamic Global Vegetation Models (DGVMs) coupled with human-related information as  
337 population density. Obtaining data for simulating the dynamic of these human-related  
338 information remain a challenge. Major efforts have been devoted to understanding land use  
339 dynamic (Prestele et al. 2017), but forest management, fire prevention and grazing practices are  
340 still the major unknown requiring better data assemblage and modeling processes (Pongratz et al.  
341 2018). In our study, we showed the strong impact of political events (here the collapse of the  
342 political regime) on grazing intensity and the subsequent effect on fire activity. These stochastic  
343 events are hard to forecast and simulate so that DGVM can capture long term trends in burned  
344 area (Yue et al. 2014, Kloster et al. 2010) when compared to observed burned area  
345 reconstructions (Mouillot and Field 2005).

346 The Russian economic collapse is unique to provide fruitful information on potential impact of  
347 grazing changes on ecosystem functioning when associated to socio-economic scenarios.  
348 Integrating grazing in DGVM has recently emerged for global models (Chang et al. 2013,  
349 Dangal et al. 2017, Pachzelt et al. 2015) and for local studies (Bachelet et al. 2000, Caracciolo et  
350 al. 2017, Vigan et al. 2017). Grazing processes can hardly capture both socio-economic scenarios  
351 and climate impact on livestock population which could be affected by climate extremes  
352 (Nandintsetseg et al. 2018) and lack of forage or water (Vrieling et al. 2016, Tachiiri and  
353 Shinoda 2012).

## 354 **5 Conclusions**

355 The spatial and temporal extent of the area burned were examined in different ecosystems in  
356 northern Eurasia from 2002 to 2016. We conclude

357 1) The burned area in grasslands declined 74 % from ~ 282,000 km<sup>2</sup> in 2002 to ~ 73,000 km<sup>2</sup> in  
358 2016 or at a rate of  $1.3 \times 10^4$  km<sup>2</sup> yr<sup>-1</sup>. The area burned in forest did not show a trend.



- 359 2) Grassland fires in Kazakhstan accounted for 47 % of the total area burned but comprised 84  
360 % of the decline of the total area burned in northern Eurasia during the 15 years.  
361 3) Wetter climate and the increase of grazing livestock in Kazakhstan are the major factors  
362 contributing to the decline of the area burned in northern Eurasia.  
363 4) Most of Kazakhstan became wetter from 2002 to 2016, decreasing high fire years due to less  
364 frequent dry years.  
365 5) The population of livestock increased in most of Kazakhstan from 2002 to 2016, decreasing  
366 the burned area during the wettest years by fuel removal from grazing.  
367 6) The major factors affecting the availability of the fuels for the decline of burned area are:  
368 climate, proportion of the grassland cover, aboveground net primary production and livestock  
369 density. These factors interact to reduce the area burned in Kazakhstan, especially in  
370 grassland.

371

372 *Data availability.* All data and materials are available in the manuscript or the supplementary  
373 materials. The original geospatial dataset of the burned area is large and will be available upon  
374 reasonable request. However, a derived dataset has been used to estimate black carbon emissions  
375 from fires in the same region. It has been archived at the Forest Service Data Archive web site  
376 (Hao et al., 2016b). <https://www.fs.usda.gov/rds/archive/Product/RDS-2016-0036/>  
377

378

379 *Supplement.* The supplement for this article is available online at: xxx.

380

381 *Author contributions.* W.M.H. led the project and led writing the manuscript. M.C.R. simulated  
382 aboveground biomass ANPP and advised statistical analysis. L.S.B. was responsible for  
383 statistical analysis. Y.B., P.C. and F.M. suggested the use of PDSI and livestock population to  
384 explain the declining burned areas. B.N. analyzed the data and contributed certain figures. A.P.  
385 mapped burned areas., R.E.C. conducted GIS analysis. S.P.U. advised the execution of the  
386 project. C.Y. advised on the trend of the burned areas. All authors contributed the writing of the  
387 manuscript

388

389 *Competing interests.* The authors do not have competing interests.

390

391 *Acknowledgements.* W.M.H. received funding from the US Department of State, US Forest  
392 Service Research and Development, and NASA Terrestrial Ecology Program. Y.B. and P.C.  
393 have received funding from the European Union's Horizon 2020 research and innovation  
394 program under grant agreement No 641816 (CRESCENDO). F.M. received funding from ESA  
395 FIRECCI program.

396

397

## 398 **References**

399

400 Abatzoglou, J. T. and Kolden, C. A.: Relationships between climate and macroscale area burned  
401 in the western United States, *International Journal of Wildland Fire*, 22, 1003–1020,  
402 <http://dx.doi.org/10.1071/WF13019>, 2013.

403 Andela, N. and van der Werf, G. R.: Recent trends in African fires driven by cropland expansion  
404 and El Niño to La Niña transition, *Nature Climate Change*, 4, 791–795, [https://doi:  
10.1038/NCLIMATE2313](https://doi:10.1038/NCLIMATE2313)., 2014.



- 404 Andela, N., Morton, D. C., Giglio, L., Chen, Y., van der Werf, G. R., Kasibhatla, P. S., DeFries,  
405 R. S., Collatz, G. J., Hantson, S., Kloster, S., Bachelet, D., Forrest, M., Lasslop, G., Li, F.,  
406 Mangeon, S., Melton, J. R., Yue, C., and Randerson, J. T.: A human-driven decline in global  
407 burned area, *Science*, 356, 1356-1362, [https:// doi: 10.1126/science.aal4108](https://doi.org/10.1126/science.aal4108), 2017.
- 408 Archibald, S., Roy, D. P., van Wilgen, B. W., and Scholes, R. J.: What limits fire? An  
409 examination of drivers of burnt area in Southern Africa, *Global Change Biology*, 15, 613-630,  
410 [doi:10.1111/j.1365-2486.2008.01754.x](https://doi.org/10.1111/j.1365-2486.2008.01754.x), 2009.
- 411 Bachelet, D., Lenihan, J. M., Daly, C., and Neilson, R. P.: Interactions between fire, grazing and  
412 climate change at Wind Cave National Park, SD, *Ecological Modelling*, 134, 229–244,  
413 <https://doi.org/10.1016/j.rama.2015.10.011>, 2000.
- 414 Brooks, M. E., Kristensen, K., van Benthem, K. J., Magnusson, A., Berg, C. W., Nielsen, A.,  
415 Skaug, H. J., Machler, M. and Bolker, B. M.: glmmTMB balances speed and flexibility  
416 among packages for zero-inflated generalized linear mixed modeling, *The R Journal*, 9(2),  
417 378-400, 2017.
- 418 Caracciolo, D., Istanbuloglu, E., and Noto, L.V.: An ecohydrological cellular automata model  
419 investigation of juniper tree encroachment in a western north American landscape,  
420 *Ecosystems*, 20, 1104-1123, <https://doi.org/10.1007/s10021-016-0096-6>, 2017
- 421 Cowtan, K. and Way, R. G.: Coverage bias in the HadCRUT4 temperature series and its impact  
422 on recent temperature trends, *Q. J. R. Meteorol. Soc.*, 140, 1935-1944,  
423 <https://doi.org/10.1002/qj.2297>, 2014.
- 424 Chang, J. F., Viovy, N., Vuichard, N., Ciais, P., Wang, T., Cozic, A., Lardy, R., Graux, A.-L., Klumpp,  
425 K., Martin, R., and Soussana, J. F.: Incorporating grassland management in ORCGIDEE: model  
426 description and evaluation at 11 eddy-covariance sites in Europe, *Geosci. Model Dev.*, 6, 2165-2181,  
427 <https://doi.org/10.5194/gmd-6-2165-2013>, 2013.
- 428 Chuvieco, E., Mouillot, F., van der Werf, G. R., San Miguel, J., Tanase, M., Koutsias, N.,  
429 García, M., Yebra, M., Padilla, M., Gitas, I., Heil, A., Hawbaker, T. J., and Giglio, L.:  
430 Historical background and current developments for mapping burned area from satellite Earth  
431 observation, *Remote Sens. Environ.*, 225, 45-64, <https://doi.org/10.1016/j.rse.2019.02.013>,  
432 2019.
- 433 Dangal, S. R. S., Tian, H., Lu, C., Ren, W., Pan, S., Yang, J., Di Cosmo, N., and Hessel, A.:  
434 Integrating herbivore population dynamics into a global land biosphere model: plugging  
435 animals into the earth system, *Journal of advances in modeling earth systems*, 9, 2920-2945,  
436 <https://doi.org/10.1002/2016MS000904>, 2017.
- 437 Dubinin, M., Luschekina, A., and Radeloff, V. C.: Climate, livestock, and vegetation: what  
438 drives fire increase in the arid ecosystems of southern Russia? *Ecosystems*, 14, 547-562,  
439 [https://doi: 10.1007/s10021-011-9427-9](https://doi.org/10.1007/s10021-011-9427-9), 2011.
- 440 Evangeliou, N., Balkanski, Y., Hao, W. M., Petkov, A., Silverstein, R. P., Corley, R., Nordgren,  
441 B. L., Urbanski, S. P., Eckhardt, S., Stohl, A., Tunved, P., Crepinsek, S., Jefferson, A.,  
442 Sharma, S., Nøjgaard, J. K., and Skov, H.: Wildfires in northern Eurasia affect the budget of  
443 black carbon in the Arctic – a 12-year retrospective synopsis (2002–2013), *Atmos. Chem.*  
444 *Phys.*, 16, 7587-7604, <https://doi.org/10.5194/acp-16-7587-2016>, 2016.
- 445 Food and Agriculture Organization FAOSTAT Live Animals Database,  
446 <http://www.fao.org/faostat/en/#home>, 2016.
- 447 Friedl, M. A., Sulla-Menashe, D., Tan, B., Schneider, A., Ramankutty, N., Sibley, A., and  
448 Huang, X.: MODIS collection 5 global land cover: algorithm refinements and characterization



- 449 of new datasets, *Remote Sens. Environ.*, 114, 168-182,  
450 <https://doi.org/10.1016/j.rse.2009.08.016>, 2010.
- 451 Fyfe, J. C., Gillett, N. P., and Zwiers, F. W.: Overestimated global warming over the past 20  
452 years. *Nature Clim Chang*, 3, 767-769, <https://doi.org/10.1038/nclimate1972>, 2013.
- 453 Gedalof, Z., Peterson, D. L., and Mantua, N. J.: Atmospheric, climatic, and ecological controls  
454 on extreme wildfire years in the northwestern United States, *Ecological Applications*, 15,  
455 154–174, <https://doi.org/10.1890/03-5116>, 2005.
- 456 Giglio, L., Boschetti, L., Roy, D., Humber, M. L., and Justice, C. O.: The collection 6 MODIS  
457 burned area mapping algorithm and product, *Remote Sens. Environ.*, 217, 72-85,  
458 <https://doi.org/10.1016/j.rse.2018.08.005>, 2018.
- 459 Giglio, L., Randerson, J. T., and van der Werf, G. R.: Analysis of daily, monthly, and annual  
460 burned area using the fourth-generation global fire emissions database (GFED4), *J. Geophys.*  
461 *Res. Biogeosci.*, 118, 317–328, doi:10.1002/jgrg.20042, 2013.
- 462 Goetz, S. J., MacK, M. C., Gurney, K. R., Randerson, J. T., and Houghton, R. A.: Ecosystem  
463 responses to recent climate change and fire disturbance at northern high latitudes:  
464 observations and model results contrasting northern Eurasia and North America, *Environ.*  
465 *Res. Lett.*, 2, 045031, <https://doi.org/10.1088/1748-9326/2/4/045031>, 2007.
- 466 Goldammer, J. G., Stocks, B. J., Sukhinin, A. I., and Ponomarev, E.: Current fire regimes,  
467 impacts and likely challenges - II: forest fires in Russia - past and current trends. in  
468 *Vegetation Fires and Global Change*, Goldammer, J. G., Ed., 51-78, 2013.
- 469 Groisman, P. Ya., Sherstyukov, B. G., Razuvaev, V. N., Knight, R. W., Enloe, J. G.,  
470 Stroumentova, N. S., Whitfield, P. H., Førland, E., Hannsen-Bauer, I., Tuomenvirta, H.,  
471 Aleksandersson, H., Mescherskaya, A. V., and Karl, T. R.: Potential forest fire danger over  
472 Northern Eurasia: Changes during the 20th century, *Global and Planetary Change*, 56, 371-  
473 386, <https://doi.org/10.1016/j.gloplacha.2006.07.029>, 2007.
- 474 Hantson, S., Arneeth, A., Harrison, S. P., Kelley, D. I., Prentice, I. C., Rabin, S. S., Archibald, S.,  
475 Mouillot, F., Arnold, S. R., Artaxo, P., Bachelet, D., Ciais, P., Forrest, M., Friedlingstein, P.,  
476 Hickler, T., Kaplan, J. O., Kloster, S., Knorr, W., Lasslop, G., Li, F., Mangeon, S., Melton, J.  
477 R., Meyn, A., Sitch, S., Spessa, A., van der Werf, G. R., Voulgarakis, A., and Yue, C.: The  
478 status and challenge of global fire modelling, *Biogeosciences*, 13, 3359-3375, DOI:  
479 10.5194/bg-13-3359-2016, 2016.
- 480 Hao, W. M. and Liu, M.-H.: Spatial and temporal distribution of tropical biomass burning,  
481 *Global Biogeochem. Cy.*, 8, 495-503, <https://doi.org/10.1029/94GB02086>, 1994.
- 482 Hao, W. M., Petkov, A., Nordgren, B. L., Corley, R. E., Silverstein, R. P., Urbanski, S. P.,  
483 Evangeliou, N., Balkanski, Y., and Kinder, B. L.: Daily black carbon emissions from fires in  
484 northern Eurasia for 2002–2015, *Geosci. Model Dev.*, 9, 4461-4474, [www.geosci-model-](http://www.geosci-model-dev.net/9/4461/2016/doi:10.5194/gmd-9-4461-2016)  
485 [dev.net/9/4461/2016/doi:10.5194/gmd-9-4461-2016](http://www.geosci-model-dev.net/9/4461/2016/doi:10.5194/gmd-9-4461-2016), 2016a.
- 486 Hao, W. M., Petkov, A., Nordgren, B. L., Corley, R. E., Silverstein, R. P., and Urbanski, S. P.:  
487 Daily black carbon emissions data from fires in Northern Eurasia for 2002–2015, *Forest*  
488 *Service Research Data Archive*, <https://doi.org/10.2737/RDS-2016-0036>, 2016b.
- 489 Holdo, R. M., Holt, R. D., and Fryxell, J. M.: Grazers, browsers, and fire influence the extent and  
490 spatial pattern of tree cover in the Serengeti, *Ecological Applications*, 19, 95-109,  
491 <https://doi.org/10.1890/07-1954.1>, 2009.
- 492 Huber, P. J.: *Statistics*, John Wiley & Sons, 1981.
- 493 IPCC, 2013: *Climate Change 2013: The Physical Science Basis*. Contribution of Working Group  
494 I to the Fifth Assessment Report of the Intergovernmental Panel on Climate Change [Stocker,



- 495 T.F., D. Qin, G.-K. Plattner, M. Tignor, S.K. Allen, J. Boschung, A. Nauels, Y. Xia, V. Bex  
496 and P.M. Midgley (eds.]. Cambridge University Press, Cambridge, United Kingdom and  
497 New York, NY, USA, 1535 pp., 2013.
- 498 IPCC, 2014: Climate Change 2014: Synthesis Report. Contribution of Working Groups I, II and  
499 III to the Fifth Assessment Report of the Intergovernmental Panel on Climate Change [Core  
500 Writing Team, R.K. Pachauri and L.A. Meyer (eds.)]. IPCC, Geneva, Switzerland, 151 pp.,  
501 2014.
- 502 Jolly, W. M., Cochrane, M. A., Freeborn, P. H., Holden, Z. A., Brown, T. J., Williamson, G. J.,  
503 and Bowman, D. M. J. S.: Climate-induced variations in global wildfire danger from 1979 to  
504 2013, *Nature communications*, 6, 7537, <https://doi.org/10.1038/ncomms8537>, 2015.
- 505 Kendall, M.: A new measure of rank correlation, *Biometrika*. 30 (1–2): 81–89, 1938.
- 506 Kharuk, V. I., Ranson, K. J., and Dvinskaya, M. L.: Wildfire dynamics in larch dominance zone,  
507 *Geophys. Res. Lett.*, 35, L01402, <https://doi.org/10.1029/2007GL032291>, 2008.
- 508 Kloster, S., Mahowald, N. M., Randerson, J. T., Thornton, P. E., Hoffman, F. M., Levis, S.,  
509 Lawrence, P. J., Feddema, J. J., Oleson, K. W., and Lawrence, D. M.: Fire dynamics during  
510 the 20<sup>th</sup> century simulated by the community land model, *Biogeosciences*, 7, 1877–1902,  
511 <https://doi.org/10.5194/bg-7-1877-2010>, 2010.
- 512 Koerner, S. E. and Collins, S. L.: Interactive effects of grazing, drought, and fire on grassland  
513 plant communities in North America and South Africa, *Ecology*, 95, 98–109,  
514 <https://doi.org/10.1890/13-0526.1>, 2014.
- 515 Krawchuck, M. A. and Moritz, M. A.: Constraints on global fire activity vary across a resource  
516 gradient, *Ecology*, 92, 121–132, <https://doi.org/10.1890/09-1843.1>, 2011.
- 517 Liu, Yi. Y., Evans, J. P., McCabe, M. F., de Jeu, R. A. M., van Dijk, A. I. J. M., Dolman, A. J.,  
518 and Saizen, I.: Changing climate and overgrazing are decimating Mongolian steppes, *PLoS*  
519 *ONE* 8, e57599, <https://doi.org/10.1371/journal.pone.0057599>, 2013.
- 520 MANE: National Economy of the Republic of Kazakhstan Committee on Statistics. 2019.  
521 [http://www.stat.gov.kz/faces/wcnav\\_externalId/homeNumbersAgriculture](http://www.stat.gov.kz/faces/wcnav_externalId/homeNumbersAgriculture). Last Visited April  
522 28, 2019.
- 523 Mondal, N. and Sukumar, R.: Fires in seasonally dry tropical forest: testing the varying  
524 constraints hypothesis across a regional rainfall gradient, *PLoS ONE*, 11, e0159691,  
525 <https://doi.org/10.1371/journal.pone.0159691>, 2016.
- 526 Moritz, M. A., Morais, M. E., Summerell, L. A., Carlson, J. M., and Doyle, J.: Wildfires,  
527 complexity, and highly optimized tolerance, *PNAS*, 102, 17912–17917,  
528 <https://doi.org/10.1073/pnas.0508985102>, 2005.
- 529 Mouillot, F. and Field, C. B.: Fire history and the global carbon budget: a 1° x 1° fire history  
530 reconstruction for the 20<sup>th</sup> century, *Global Change Biology*, 11, 398–420,  
531 <https://doi.org/10.1111/j.1365-2486.2005.00920.x>, 2005.
- 532 Mouillot, F., Schultz, M. G., Yue, C., Cadule, P., Tansey, K., Ciais, P., and Chuvieco, E.: Ten  
533 years of global burned area products from spaceborne remote sensing - a review: analysis of  
534 user needs and recommendations for future developments, *International Journal of Applied*  
535 *Earth Observation and Geoinformation*, 2014, 26, 64–79,  
536 <https://doi.org/10.1016/j.jag.2013.05.014>, 2014.
- 537 Nandintsetseg, B., Shinoda, M., Du, C., and Munkhjargal, E: Cold-season disasters on the  
538 Eurasian steppes: climate-driven or man-made, *Scientific reports*, 8, 15905,  
539 <https://doi.org/10.1038/s41598-018-33046-1>, 2018.

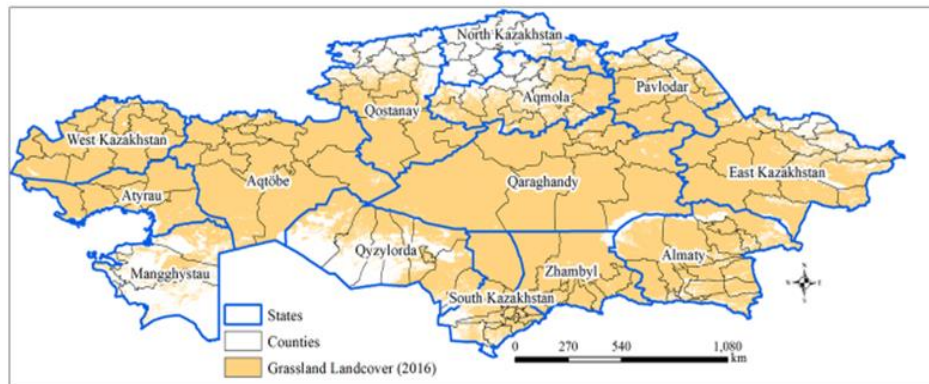


- 540 NASA Global Climate Change, <https://climate.nasa.gov/vital-signs/global-temperature/>, last  
541 access, September 12, 2019.
- 542 Official Agriculture Statistics of Kazakhstan,  
543 [http://www.stat.gov.kz/faces/wcnav\\_externalId/homeNumbersAgriculture](http://www.stat.gov.kz/faces/wcnav_externalId/homeNumbersAgriculture), 2016.
- 544 Otón, G., Ramo, R., Lizundia-Loiola, J., and Chuvieco, E.: Global detection of long-term (1982–  
545 2017) burned area with AVHRR-LTDR data, *Remote Sens.*, 11, 2079,  
546 <https://doi.org/10.3390/rs11182079>, 2019.
- 547 Pachzelt, A., Forrest, M., Ramming, A., Higgins, S. I., and Hickler, T.: Potential impact of large  
548 ungulate grazers on African vegetation, carbon storage and fire regimes, *Global ecology and*  
549 *biogeography*, 24, 991–1002, <https://doi.org/10.1111/geb.12313>, 2015.
- 550 Palmer, W., Meteorological drought, U.S. Department of Commerce, Weather Bureau, Research  
551 Paper, 45, 1965.
- 552 Pausas, J. G. and Ribeiro, E.: The global fire-productivity relationship, *Global ecology and*  
553 *biogeography*, 22, 728–736, <https://doi.org/10.1111/geb.12043>, 2013.
- 554 Pongratz, J., Dolman, H., Don, A., Erb, K.-H., Fuchs, R., Herold, M., Jones, C., Kuemmerle, T.,  
555 Luyssaert, S., Meyfroidt, P., and Naudts, K.: Models meet data: Challenges and opportunities  
556 in implementing land management in earth system models. *Global change biology*, 24, 1470–  
557 1487, <https://doi.org/10.1111/gcb.13988>, 2018.
- 558 Prestele, R., Arneth, A., Bondeau, A., De Noblet-Ducoudre, N., Pugh, T. A. M., Sitch, S.,  
559 Stehfest, E., and Verburg, P. H.: Current challenges of implementing anthropogenic land-use  
560 and land-cover change in models contributing to climate change assessments, *Earth system*  
561 *dynamics*, 8, 369–386, doi:10.5194/esd-8-369-2017, 2017.
- 562 R Core Team: R: A language and environment for statistical computing. R Foundation for  
563 Statistical Computing, Vienna, Austria. URL <https://www.R-project.org/>, 2019.
- 564 Reeves, M. C.: Development of the rangeland vegetation simulator: A module of the forest  
565 vegetation simulator. Final report to the Joint Fire Science Program, Boise, Idaho, 2016.
- 566 Riley, K. L., Abatzoglou, J. T., Grenfell, I. C., Klene, A. E., and Heinsch, F. A.: The relationship  
567 of large fire occurrence with drought and fire danger indices in the western USA, 1984–2008,  
568 *International Journal of Wildland Fire*, 22, 894–909, <https://doi.org/10.1071/WF12149>,  
569 2013.
- 570 Robinson, S. and Milner-Gulland, E. J.: Political change and factors limiting numbers of wild  
571 and domestic ungulates in Kazakhstan, *Human Ecology*, 31, 87–110,  
572 <https://doi.org/10.1023/A:1022834224257>, 2003.
- 573 Roy, D. P., Boschetti, L., Justice, C.O., and Ju, J.: The collection 5 MODIS burned area product  
574 – global evaluation by comparison with the MODIS active fire product, *Remote Sens.*  
575 *Environ.*, 112, 3690–3707, <https://doi.org/10.1016/j.rse.2008.05.013>, 2008.
- 576 Scheiter, S. and Savadogo, P.: Ecosystem management can mitigate vegetation shifts induced by  
577 climate change in West Africa, *Ecological Modelling*, 332, 19–27,  
578 <https://doi.org/10.1016/j.ecolmodel.2016.03.022>, 2016.
- 579 Seneviratne, S. I., Donat, M. G., Mueller, B., and Alexander, L.V.: No pause in the increase of  
580 hot temperature extremes, *Nature Climate Change*, 4, 161–163,  
581 <https://doi.org/10.1038/nclimate2206>, 2014.
- 582 Tachiiri, K and Shinoda, M.: Quantitative risk assessment for future meteorological disasters  
583 reduced livestock mortality in Mongolia, *Climatic Change*, 113, 867–882,  
584 <https://doi.org/10.1007/s10584-011-0365-5>, 2012.



- 585 Trenberth, K. E., Fasullo, J. T., Branstator, G., and Phillips, A. S.: Seasonal aspects of the recent  
586 pause in surface warming, *Nature Climate Change*, 4, 911-916,  
587 <https://doi.org/10.1038/nclimate2341>, 2014.
- 588 Trenberth, K. E., Fasullo, J. T., and Shepherd, T. G.: Attribution of climate extreme events,  
589 *Nature Climate Change*, 5, 725-730, <https://doi.org/10.1038/nclimate2657>, 2015.
- 590 Vandergert, P. and Newell, J. P.: Illegal logging in the Russian Far East and Siberia, *Int. For.*  
591 *Rev.*, 5, 303-306, <https://doi.org/10.1505/IFOR.5.3.303.19150>, 2003.
- 592 Venables W. N. and Ripley, B. D.: *Modern Applied Statistics with S*, Fourth edition. Springer,  
593 New York. ISBN 0-387-95457-0, 2002.
- 594 Vigan, A., Lasseur, J., Benoit, M., Mouillot, F., Eugène, M., Mansard, L., Vigne, M., Lecomte,  
595 P., and Dutilly, C.: Evaluating livestock mobility as a strategy for climate change mitigation:  
596 combining models to address the specificities of pastoral systems, *Agriculture Ecosystems*  
597 *and Environment*, 242, 89-101, <https://doi.org/10.1016/j.agee.2017.03.020>, 2017.
- 598 Vrieling, A., Meroni, M., Mude, A. G., Chantarat, S., Ummenhofer, C. C., and de Bie, K.: Early  
599 assessment of seasonal forage availability for mitigating the impact of drought on East  
600 African pastoralists, *Remote Sens. Environ.*, 174, 44-55,  
601 <https://doi.org/10.1016/j.rse.2015.12.003>, 2016.
- 602 Xu, Y., Zhang, Y., Chen, J., and Ranjeet, J.: Livestock dynamics under changing economy and  
603 climate in Mongolia, *Land Use Policy*, 88, 104120,  
604 <https://doi.org/10.1016/j.landusepol.2019.104120>, 2019.
- 605 Yue, C., Ciais, P., Cadule, P., Thonicke, K., Archibald, S., Poulter, B., Hao, W. M., Hantson, S.,  
606 Mouillot, F., Friedlingstein, P., Maignan, F., and Viovy, N.: Modelling the role of fires in the  
607 terrestrial carbon balance by incorporating SPITFIRE into the global vegetation model  
608 ORCHIDEE- part 1: simulating historical global burned area and fire regimes. *Geosci. Model*  
609 *Dev.*, 7, 2747-2767, <https://doi.org/10.5194/gmd-7-2747-2014>, 2014.

610



611

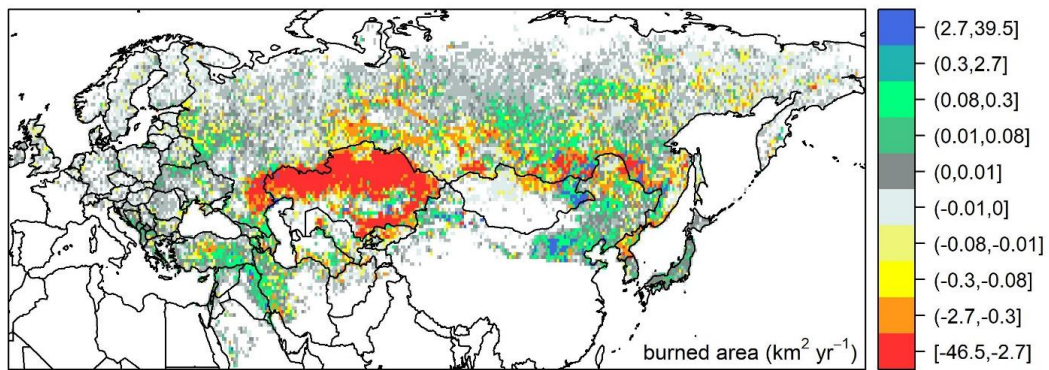
612 **Figure 1.** The distribution of grassland cover in Kazakhstan with counties and states shown as  
613 administrative boundaries.

614

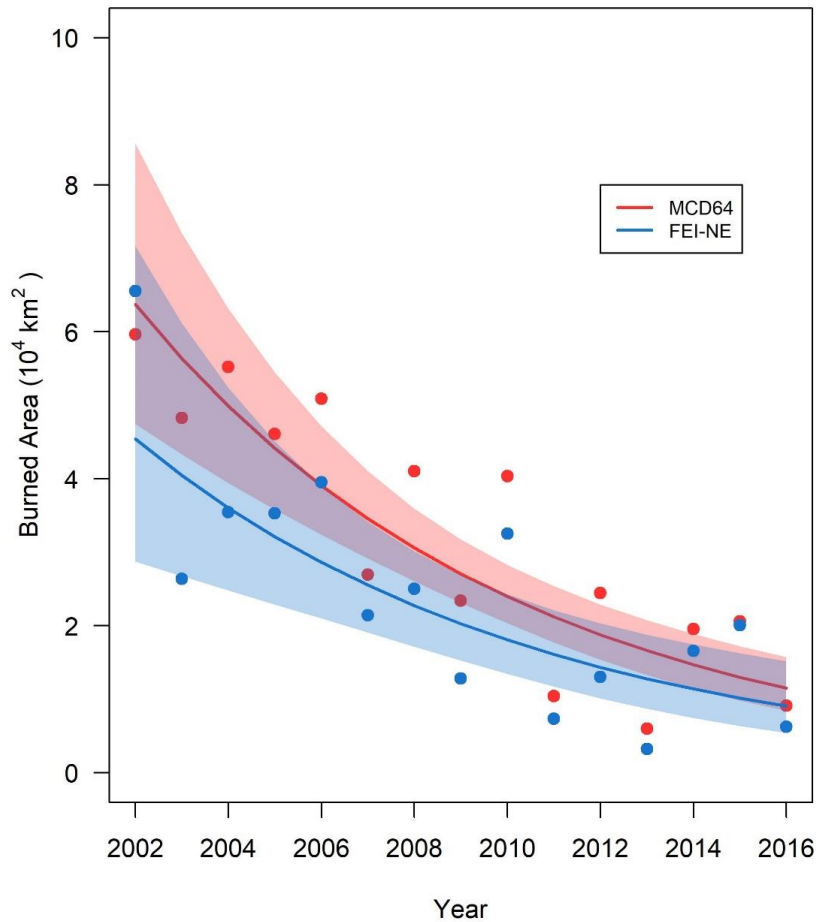
615

616





617  
618 **Figure 2.** Spatial distributions of robust linear trends of the area burned for each  $0.5^\circ \times 0.5^\circ$  grid  
619 cell in northern Eurasia from 2002 to 2016.  
620  
621  
622  
623  
624  
625  
626  
627  
628  
629  
630  
631  
632

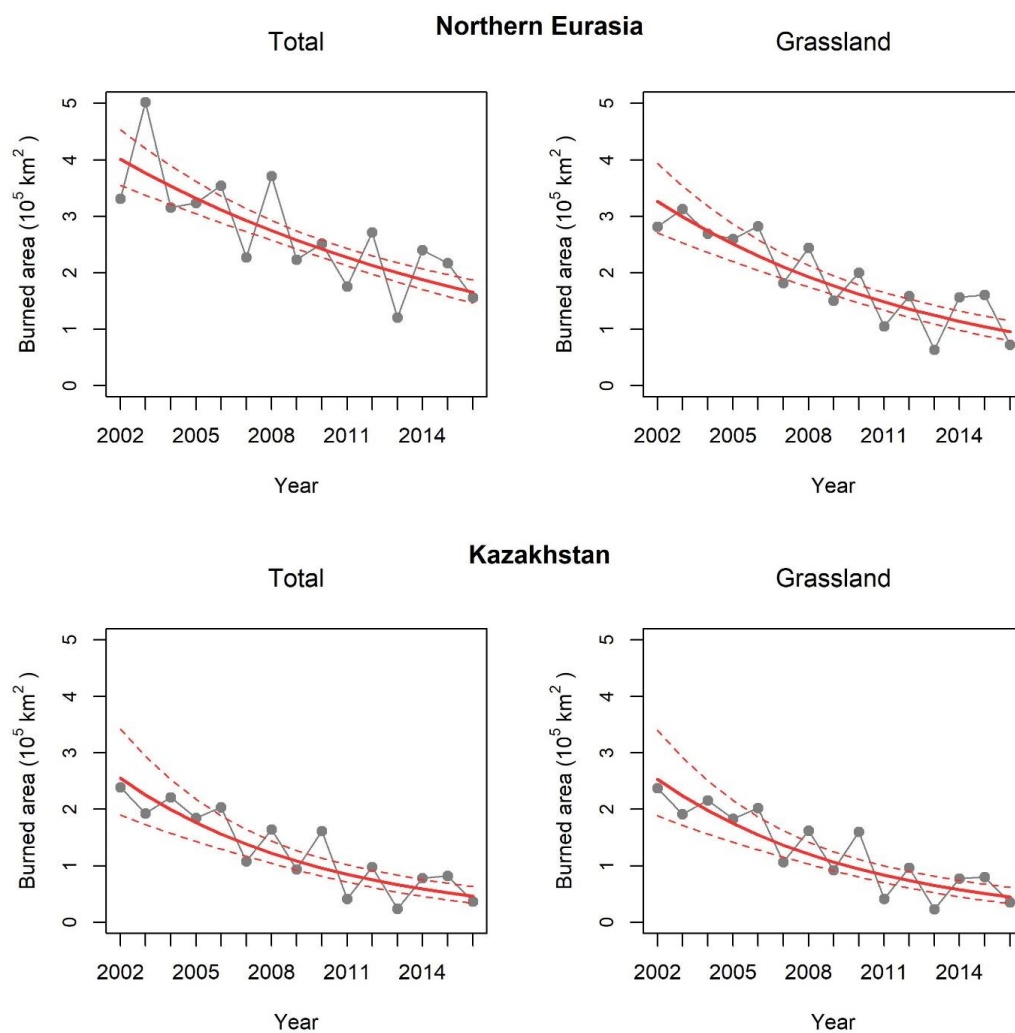


633

634 **Figure 3.** Comparison of burned areas between the dataset of Forest Service Fire Emission  
635 Inventory – northern Eurasia (FEI-NE) and MODIS MCD64. The FEI-NE (blue) and MCD64  
636 (pink) bands illustrate the 95% confidence intervals.



637



638

639

640

641

642

**Figure 4.** Declining trends of the total area and grassland area burned in northern Eurasia and Kazakhstan from 2002 to 2016. The solid lines are the trend lines and the dotted lines are 95% confidence intervals.

643

644

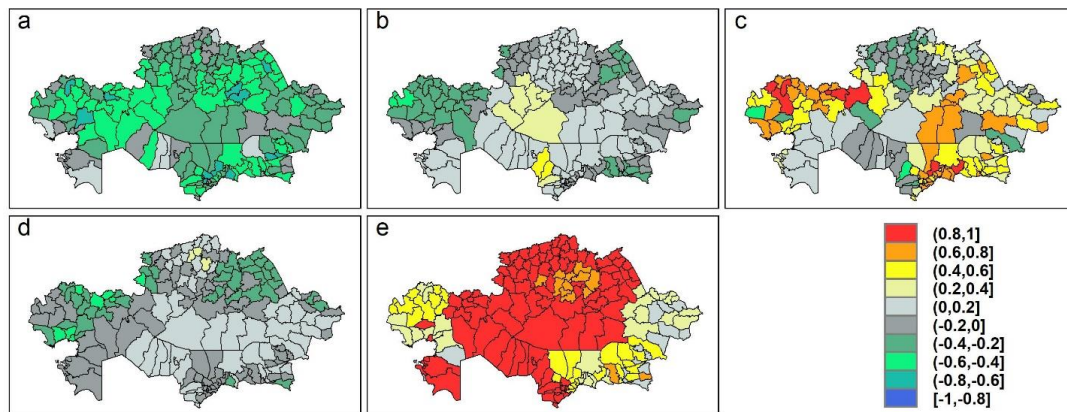
645

646

647

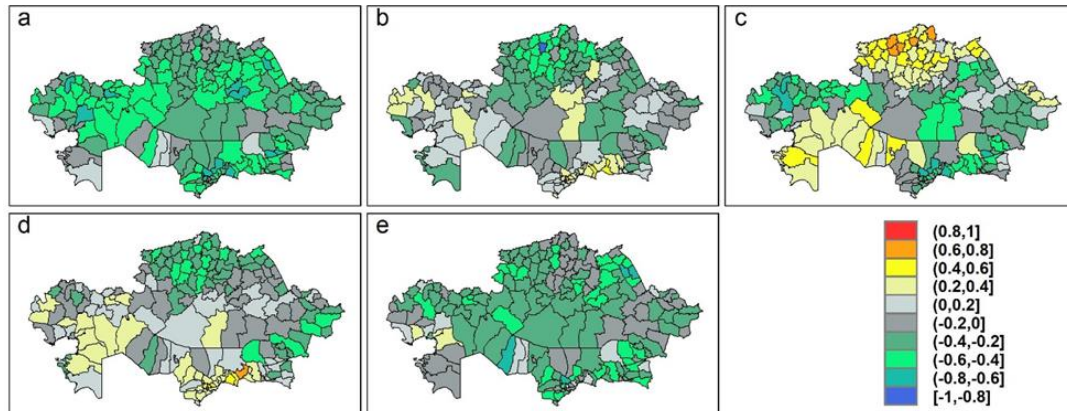
648

649



650  
651  
652  
653  
654  
655

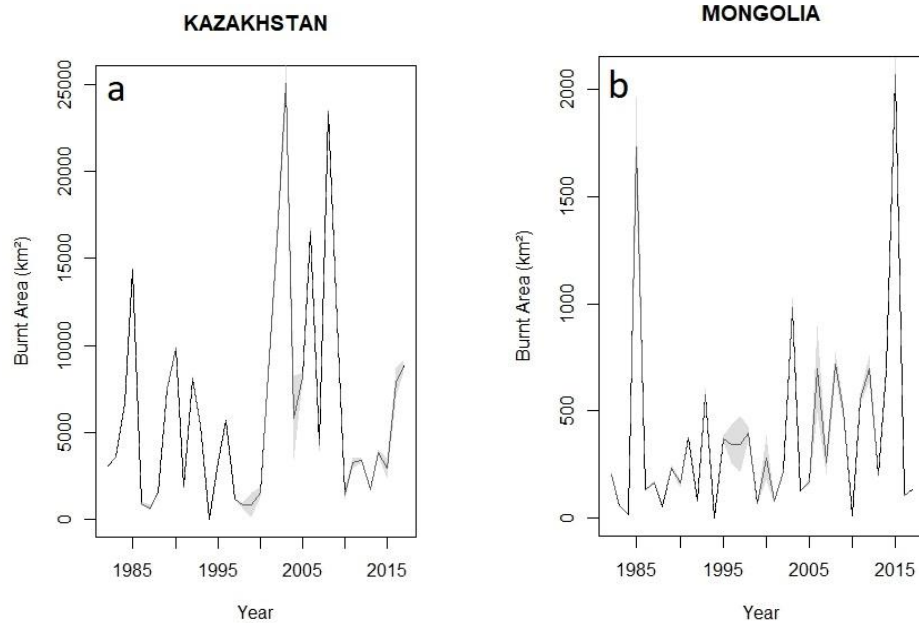
**Figure 5.** Pairwise robust rank correlations of year with (a) fraction of burned area, (b) PDSI, (c) proportion of grassland layer, (d) ANPP and (e) livestock density without considering their interactions.



656  
657

658 **Figure 6.** Pairwise robust rank correlations of fraction of burned area with (a) year, (b) PDSI, (c)  
659 proportion of grassland layer, (d) ANPP and (e) livestock density without considering their  
660 interactions.

661  
662  
663  
664  
665  
666  
667  
668  
669  
670  
671  
672  
673  
674  
675  
676  
677  
678  
679  
680  
681  
682  
683  
684  
685



686  
687 **Figure 7.** Yearly burned area (in km<sup>2</sup>) in (a) Kazakstan and (b) Mongolia for the 1982-2017  
688 periode based on the AVHRR remotely sensed burned area Long Term Data Record\_Climatte  
689 Change Initiative (FIRECCILT10) (<https://www.mdpi.com/2072-4292/11/18/2079>, Otón et al.,  
690 2019). Black line represents mean burned fraction and grey area the burned area 95% uncertainty  
691 delivered by FIRECCILT10  
692



**Table 1.** The area burned in forest, grassland, shrubland and savanna in geographic regions from 2002 to 2016. The data of the area burned in Kazakhstan are listed for comparison only, and are not included in the tabulation.

Region	Burned Area (km <sup>2</sup> )															
	2002	2003	2004	2005	2006	2007	2008	2009	2010	2011	2012	2013	2014	2015	2016	Total
<b>Forest (Evergreen Needleleaf, Evergreen Broadleaf, Deciduous Needleleaf, Deciduous Broadleaf, Mixed)</b>																
Russia	26,458	99,944	16,715	20,561	32,929	23,731	72,671	33,356	19,309	43,910	73,920	29,791	62,701	38,511	51,718	646,223
East Asia	1,483	9,697	6,368	4,202	2,814	2,524	4,597	6,676	1,258	3,379	4,189	1,819	3,151	2,944	1,336	56,436
Central & Western Asia	131	206	367	259	388	469	641	389	348	159	321	307	517	726	455	5,684
Europe	376	1,172	467	592	491	1,170	850	863	328	1,206	2,307	537	1,224	1,756	575	13,911
Subtotal	28,448	111,019	23,917	25,613	36,623	27,894	78,758	41,283	21,243	48,653	80,736	32,455	67,592	43,937	54,084	722,254
<b>Grassland</b>																
Russia	32,019	97,754	33,372	61,755	62,973	55,220	65,144	46,375	30,634	43,760	37,261	21,114	51,745	49,857	22,178	711,160
East Asia	10,643	21,235	15,551	12,433	14,456	16,819	15,278	11,259	8,097	18,716	23,870	18,123	26,689	29,361	13,962	256,492
Central & Western Asia	239,160	193,580	220,080	185,531	204,627	109,248	163,814	92,592	161,668	41,943	97,363	24,364	78,203	81,517	36,369	1,930,057
Europe	128	271	108	555	241	616	325	217	104	401	526	150	186	237	179	4,242
Subtotal	281,948	312,840	269,112	260,273	282,296	181,903	244,560	150,443	200,503	104,819	159,021	63,752	156,822	160,972	72,688	2,901,951
Kazakhstan	237,335	191,466	215,977	182,968	202,292	106,558	162,474	91,873	160,318	40,995	96,420	23,195	76,977	80,251	35,249	1,904,348
<b>Shrubland (Closed Shrubland and Open Shrubland)</b>																
Russia	7,042	27,749	4,894	13,149	5,924	2,868	10,901	13,096	18,854	6,697	12,650	10,918	5,717	3,486	14,529	158,470
East Asia	337	79	264	828	934	675	790	645	375	914	796	193	317	153	191	7,490
Central & Western Asia	1,022	2,836	5,632	2,384	1,255	1,728	999	1,217	3,279	964	769	845	1,066	1,287	1,720	27,001
Europe	20	38	23	70	39	121	112	87	21	83	70	11	13	10	17	732
Subtotal	8,421	30,701	10,813	16,430	8,152	5,391	12,802	15,044	22,529	8,657	14,285	11,966	7,112	4,934	16,457	193,693
<b>Savanna (Woody Savanna and Savanna)</b>																
Russia	11,136	43,574	8,307	19,343	25,129	10,465	33,347	14,191	6,745	12,473	16,387	12,076	8,324	6,261	12,039	239,796
East Asia	589	3,504	3,257	1,275	1,564	694	1,268	1,349	465	611	660	205	147	510	131	16,226
Central & Western Asia	575	500	437	395	442	317	413	391	261	115	193	112	161	301	178	4,791
Europe	83	207	110	293	200	653	340	400	113	319	426	212	201	142	243	3,941
Subtotal	12,383	47,785	12,110	21,306	27,335	12,128	35,368	16,330	7,584	13,517	17,666	12,604	8,832	7,215	12,592	264,753
Total	331,199	502,346	315,951	323,621	354,405	227,317	371,488	223,100	251,859	175,646	271,707	120,777	240,358	217,058	155,820	4,082,650



**Table 2.** Model parameters and associated *p*-values.

<i>Parameter</i>	<i>Estimate</i>	<i>Std. Error</i>	<i>z</i>	<i>Pr(&gt; z )</i>
Year * ANPP	-0.02	0.01	-4.03	<0.001
Year * PDSI	0.00	0.00	0.20	0.838
Year * Proportion Grass Area	-0.26	0.04	-6.77	<0.001
Year * Livestock Density (head km <sup>-2</sup> )	1.04	0.61	1.70	0.089
ANPP * PDSI	-0.01	0.01	-0.92	0.360
ANPP * Proportion Grass Area	0.72	0.19	3.83	<0.001
ANPP * Livestock Density (head km <sup>-2</sup> )	0.88	3.22	0.27	0.784
PDSI * Proportion Grass Area	-0.24	0.11	-2.20	0.028
PDSI * Livestock Density (head km <sup>-2</sup> )	-3.30	1.62	-2.04	0.042
Proportion Grass Area * Livestock Density (head km <sup>-2</sup> )	37.78	28.32	1.33	0.182

Estimate = parameter estimate from GLMM, Std. Error = standard error of parameter estimate, z = z-statistic, Pr(>|z|) = p-value.